Journal of Applied Mechanics and Technical Physics, Vol. 42, No. 1, pp. 14–20, 2001

SHOCK COMPRESSION OF A PLATE ON A WEDGED-SHAPED TARGET

A. A. Charakhch'yan

UDC 537.84

Problems of compression of a plate on a wedge-shaped target by a strong shock wave and plate acceleration are studied using the equations of dissipationless hydrodynamics of compressible media. The state of an aluminum plate accelerated or compressed by an aluminum impactor with a velocity of 5–15 km/sec *is studied numerically. For a compression regime in which a shaped-charge jet forms, critical values of the wedge angle are obtained beginning with which the shaped-charge jet is in the liquid or solid state and does not contain the boiling liquid. For the jetless regime of shock-wave compression, an approximate solution with an attached shock wave is constructed that takes into account the phase composition of the plate material in the rarefaction wave. The constructed solution is compared with the solution of the original problem. The temperature behind the front of the attached shock wave was found to be considerably (severalfold) higher than the temperature behind the front of the compression wave. The fundamental possibility of initiating a thermonuclear reaction is shown for jetless compression of a plate of deuterium ice by a strong shock wave.*

Introduction. In the present paper, we consider the following problem. A wedge-shaped lead target and a plate of a different material form angle φ (Fig. 1). A shock wave is generated on the external surface of the target by an aluminum impactor which collides with the plate with velocity v. The initial compression stage is examined in which the plate has not yet completely penetrated into the target. The problem is solved using the hydrodynamic equations for compressible media and the equations of state that are valid over a broad range of parameters [1]. Viscosity and thermal conductivity are neglected.

The present problem is similar to the well-known problem of plate acceleration with velocity v, which is considered in theoretical studies of shaped-charge jets and conditions of their formation (see, for example, [2–7]). Two types of flow are possible (Fig. 2). For large values of φ, a shaped-charge jet of the plate material forms along the target (Fig. 2a). For small φ, there is a jetless regime of compression (Fig. 2b). After conversion to a moving coordinates system attached to the moving point of contact A (Fig. 2b), the flow becomes nearly stationary with a stream of the plate material incident on the point of contact and an attached shock wave, which causes motion of the stream along the target. The critical value $\varphi = \varphi_*$ beginning with which a shaped-charge jet arises is determined from the condition of existence of a stationary shock wave.

In contrast to the problem of plate acceleration, in the problem of plate compression by a shock wave, the flow in the plate away from the target is determined by the rarefaction wave and, thus, is not homogeneous. Moreover, in the case of a strong shock wave, the phase composition of the target material varies. Figure 3 gives the isentropes of aluminum in the plane "density–temperature" obtained from the tabulated equation of state used in the calculations. The entropy increases with increase in the temperature for fixed density. The regions corresponding to different phase states are also indicated here. On each isentrope, the pressure increases with increase in the density, and the point with minimum density corresponds to atmospheric pressure. Thus, each isentrope determines unloading of material particles with specified entropy in the

Computer Center, Russian Academy of Sciences, Moscow 117967. Translated from Prikladnaya Mekhanika i Tekhnicheskaya Fizika, Vol. 42, No. 1, pp. 17–24, January–February, 2001. Original article submitted January 10, 2000.

 0021-8944/01/4201-0014 $25.00

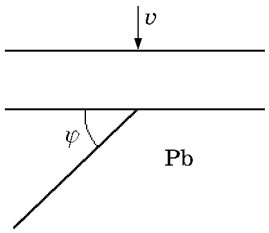

Fig. 1

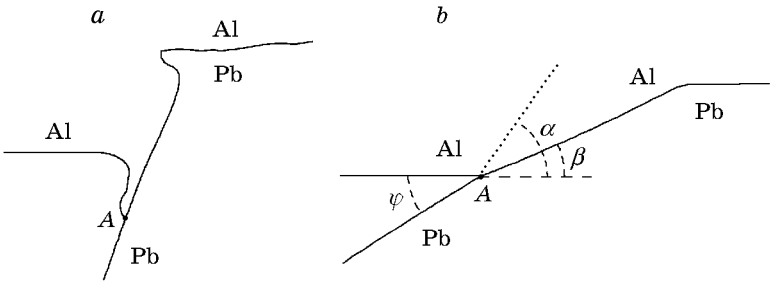

Fig. 2

Fig. 1. Diagram of the problem.

Fig. 2. Types of flow: (a) flow with a shaped-charge jet; (b) jetless flow (the dotted line is the attached shock wave).

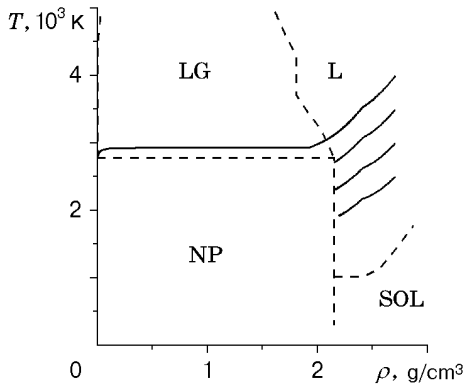

Fig. 3. Isentropes (solid curves) and phase composition of aluminum: SOL is the solid body, L is the liquid, LG is the boiling liquid, and NP is the nonphysical region.

rarefaction wave. It is obvious that there is a critical value of the entropy $S_{\rm cr}$ above which unloading of the material proceeds with formation of a region of phase equilibrium between the liquid and the gas, i.e., the boiling liquid. For the case of an aluminum plate and an aluminum impactor, the critical entropy in the shock wave corresponds to an impactor velocity of $v \approx 11$ km/sec.

We used the equations of state for the materials in the form of tabulated dependences of the pressure p and the internal energy ε on the temperature T and the density ρ. The dependences for deuterium were constructed using the dependences for hydrogen $p_{\rm H}(T,\rho)$ and $\varepsilon_{\rm H}(T,\rho)$ by the formulas

$$p(T,\rho) = p_{\rm H}(T,\rho/2), \qquad \varepsilon(T,\rho) = \varepsilon_{\rm H}(T,\rho/2)/2.$$

The hydrodynamic equations are calculated using the same software package as in [8–10]. The interfaces are distinguished explicitly in the form of lines of a curvilinear moving grid, and quasimonotonic schemes of second-order accuracy are employed. The procedure of [11] was used for suppression of entropy computation traces.

Shaped-Charge Jets. Experiments on explosive initiation of the (D–D) reaction in conical targets are described in [7, 12, 13], and results of numerical modeling are given in [8–10]. In these experiments, ring shaped-charge jets arose, which collapsed on the symmetry axis and, in the initial stage, differed little from plane jets. For experimental parameter values with a rather low neutron yield, numerical solution of the hydrodynamic equations gives a shaped-charge jet of the boiling liquid, which appears to be the reason of jet fracture. In experiments with a large neutron yield jets in the solid or liquid state arose with a small magnitude of the tensile stress inside the jet.

Chou et al. [5] obtained a criterion for the formation of a continuous jet or a dispersed jet by analysis

TABLE 1

φ, deg	M	$p_{\min}$, GPa
70	0.72	−0.7
65	0.93	−0.9
62.5	1.03	−4.4
60	1.15	−5.4
55	1.4	−6
50	1.67	−4.4

TABLE 2

v, km/sec	φ_{lg}, deg		$\mathrm{M}(\varphi_{lg})$		$\varphi_*^{\mathrm{calc}}$, deg		$\varphi_*^{\mathrm{appr}}$, deg	
	acceleration	impact	acceleration	impact	acceleration	impact	acceleration	impact
5	35	35	1.4	1.45	25	25	21.5	22
7.5	40	45	1.8	1.5	30	30	26	27.5
10	50	67.5	1.7	0.94	32.5	32.5	29.5	31
12.5	55	—	1.7	—	37.5	35	32	33.5
15	65	—	1.4	—	37.5	37.5	34	36

of experimental data and calculation results for jets produced by collision of plates. The critical value of the angle φ for which the jet characteristics change is the value for which the Mach number M of the flow incident on the point of contact is equal to 1. This is confirmed in [5] by calculations both allowing for and ignoring jet fracture within the framework of a certain model. In the last case, at $\mathrm{M} > 1$, considerable negative pressures arose in the base of the jet. Table 1 gives the dependence of the maximum magnitude of negative pressure in the jet $p_{\min}$ and the Mach number M on the angle φ obtained in the present work for the problem of acceleration of an aluminum plate with a velocity of 10 km/sec. The calculation results agree with those in [5]. For $\mathrm{M} \approx 1$, the value of $p_{\min}$ in a small range of the angle φ changes by a factor of about 5. Therefore, the criterion of [5] is also valid for the present problem.

Table 2 gives the values of the angle φ_{lg} beginning with which there is no boiling liquid in the jet and the corresponding values of the Mach number $\mathrm{M}(\varphi_{lg})$ versus the plate velocity (for the acceleration problem) and an impact velocity of 5–15 km/sec (for the problem of impact on the plate). The absence of the boiling liquid does not imply that the jet is continuous because jet fracture can occur as a result of large tensile stresses in the solid or liquid state. The results obtained supplement the well-known result of [5] on the dispersion of jets for hypersonic flow incident on the point of contact. For an impact velocity of $v > v_{\mathrm{cr}} \approx 11$ km/sec, rarefaction of the shock wave proceeds with formation of the boiling liquid. Apparently, in this case, the boiling liquid will be present in the shaped-charge jet for any value of φ. Therefore, Table 2 does not give the corresponding values of the angle φ_{lg}.

In the neighborhood of the point of contact, the solution of the problem of plate acceleration approaches a certain stationary solution with time (see, for example, [5]). Obviously, if φ_{lg} is determined from this stationary solution, then $\mathrm{M}(\varphi_{lg}) > 1$ because $\mathrm{M}(\varphi) \leqslant 1$ implies that the stationary solution is isentropic. At the initial compression stage, the flow always contain shock waves, and, therefore, the condition $\mathrm{M}(\varphi_{lg}) > 1$ is generally is not obvious. Nevertheless, as follows from Table 2, this condition is satisfied in almost all cases. According to the criterion of [5], this implies that the real jet is also dispersed for $\varphi > \varphi_{lg}$. Therefore, the problem of what changes occur in the real jet with change in φ in the neighborhood of φ_{lg} is beyond the scope of the present work and requires experimental studies. An exception is the case of impact on the plate with a velocity of 10 km/sec, which is close to v_{cr} for $\mathrm{M}(\varphi_{lg}) < 1$. In this case, transition from a continuous jet to a dispersed jet occurs for $\varphi \approx \varphi_{lg}$.

Jetless Compression. Before considering the problem of shock-wave compression of the plate, we construct an approximate solution of the problem of plate acceleration with velocity v. It is assumed that

after conversion to a moving coordinate system attached to the point of contact, there is a stationary solution with an attached shock wave (see Fig. 2b). In this coordinate system, a homogeneous flow of the plate material is incident from the left on the point of contact with velocity $v/\tan\varphi$, and the target material flow moves with velocity $v/\sin\varphi$ along the target.

Let us consider a homogeneous flow of material with density ρ_0, pressure p_0, and velocity v_0. The parameters behind the front of an oblique shock wave, in particular, the angle of rotation of the flow θ, are uniquely determined by the slope of the shock wave α and the equations of state. The corresponding dependence is denoted by $\Theta(\rho_0, p_0, v_0, \alpha)$. Solving the equation

$$\Theta(\rho_0, p_0, v_0, \alpha) = \theta \tag{1}$$

for α, one obtains the dependence of the flow parameters behind the shock-wave front on the angle θ. The corresponding dependence for pressure is denoted by $P(\rho_0, p_0, v_0, \theta)$.

Let us return to the problem of plate acceleration. We denote the slope of the target behind the point of contact by β (see Fig. 2b). The shock wave in the plate rotates the flow through angle β, and the shock wave in the target rotates the flow through angle $\varphi - \beta$. The condition of equality of the pressures in the plate and the target gives the following equation for β:

$$P_{\rm pl}(\rho_0^{\rm pl}, p_0^{\rm pl}, v/\tan\varphi, \beta) = P_{\rm t}(\rho_0^{\rm t}, p_0^{\rm t}, v/\sin\varphi, \varphi - \beta), \tag{2}$$

where the subscripts and superscripts "pl" and "t" correspond to the plate and target, respectively. The solution of Eqs. (1) and (2) was found by exhaustion of values for the variables α [for Eq. (1)] and β [for Eq. (2)] with a small step.

As is known (see, for example, [14]), for Eq. (1) there is a limiting value θ_* that restricts the region of existence of solutions of this equation to the interval $0 < \theta < \theta_*$, on which Eq. (1) has two solutions. The solution with the smaller α and smaller pressure behind the wave front is usually called a shock wave of the weak family. The second solution is called a shock wave of the strong family. Different combinations of solutions (1) for the plate and impactor give four equations of the form (2), which will be denoted by two characters: SS, SW, WS, and WW. The first character corresponds to the plate, and the second corresponds to the target; S denotes the strong family and W denotes the weak family. A numerical study of these equations shows that only the equation WW has a solution on the interval $0 < \varphi < \varphi_*^{\rm appr}$, where $\varphi_*^{\rm appr}$ is determined by the limiting value θ_* for the plate. The equations WS and SS do not have solutions, and the equation SW has a solution only on the small interval $0 < \varphi_1 < \varphi < \varphi_*^{\rm appr}$, which is bounded from below. The results given below are obtained using Eq. (2) of the WW type.

Let us consider the problem of shock-wave compression of the plate. The flow in the plate away from the target is determined by the rarefaction wave, in which the thermodynamic functions vary along the isentrope corresponding to the entropy behind the shock-wave front. The velocity of the material in the rarefaction wave as a function of the pressure p has the form

$$v(p) = u_{\rm c} + \int\limits_{p_{\rm c}}^{p} \frac{dp}{a(p, \rho(p))}, \tag{3}$$

where $u_{\rm c}$ and $p_{\rm c}$ are the velocity and pressure behind the shock-wave front, respectively, $a(p, \rho)$ is the mass velocity of sound, and the function $\rho(p)$ is determined by the isentrope.

As an approximate solution of the problem we take a solution of Eq. (2) in which $(\rho_0^{\rm pl}, p_0^{\rm pl})$ is the point lying on the corresponding isentrope and $v = v(p_0^{\rm pl})$ is the velocity defined by formula (3). If the shock-wave entropy S is smaller than the critical value $S_{\rm cr}$, i.e., upon unloading to atmospheric pressure p_0, the material remains in the liquid or solid states (see Fig. 3), it is assumed that $p_0^{\rm pl} = p_0$. For $S > S_{\rm cr}$, as $(\rho_0^{\rm pl}, p_0^{\rm pl})$, we use the point of intersection of the isentrope with the liquid-phase boundary. For the isentrope shown in Fig. 3, this point lies on the interface between the liquid and the boiling liquid. With increase in the shock-wave intensity, the boiling liquid region on the segment of the corresponding isentrope disappears, and the point $(\rho_0^{\rm pl}, p_0^{\rm pl})$ falls on the liquid–gas interface.

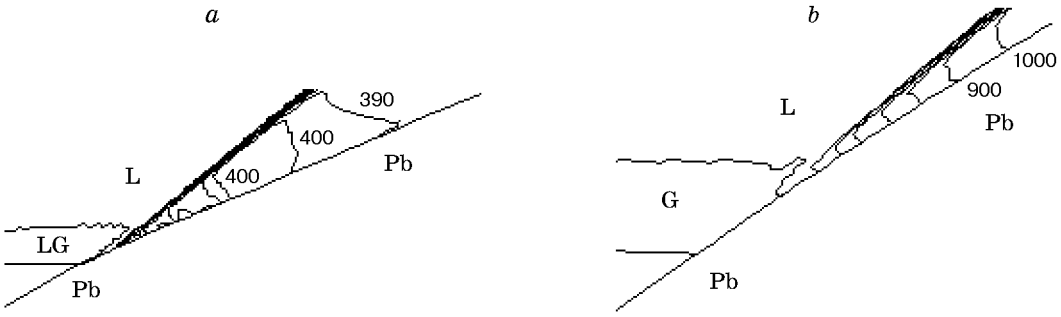

Fig. 4. Isobars (in gigapascals) and interfaces near the point of contact (L is the liquid, LG is the boiling liquid, and G is the gas) for aluminum plate ($\varphi = 30°$ and $v = 15$ km/sec) (a) and deuterium plate ($\varphi = 35°$ and $v = 50$ km/sec) (b).

TABLE 3

v, km/sec	φ, deg	β_{calc}, deg	β_{appr}, deg	α_{calc}, deg	α_{appr}, deg	p_{calc}, GPa	p_{appr}, GPa	T_{calc}, 10^3 K	T_{appr}, 10^3 K
5	20	15	13	43	47.4	98	102	3.5	3.85
7.5	25	17	17.2	46	47.2	165	171	7.6	9.6
	20	15	13.9	34	34	159	160	7.3	8.7
10	30	21.5	21.2	50	52.7	240	250	16	20
	25	18	17.9	37	38.7	230	237	16	18.4
	20	16	14.2	30	29	230	235	15	18.1
	15	10	10.6	20	21	240	235	15	18.2
12.5	30	21	21.6	42	46	310	330	30	30.8
	25	19	18	33	35	310	320	30	30.2
15	32.5	25	24.2	43	47.2	390	397	44	49
	30	23	22.3	40	41.5	400	394	42	48.7
	25	17	18.5	30	32.5	430	398	42	49

The choice of the point $(\rho_0^{\text{pl}}, p_0^{\text{pl}})$ described above is based on calculation results, according to which the attached shock wave arises in the liquid phase, i.e., it is attached to the target above the point of contact of the plate free boundary the with the target, as shown in Fig. 4 for compression of an aluminum plate and a plate of deuterium ice by a rather strong shock waves. In the case of aluminum (Fig. 4a), the isentrope of the material compressed in the shock wave passes through the boiling liquid state, and in the case of deuterium (Fig. 4b), it passes through the gas phase, which is a completely ionized plasma in this case.

We compare the approximate solution with the calculation of the hydrodynamic equations for the case of an aluminum plate. The critical values of the angle φ are given in the last four columns of Table 2. The angle φ_*^{calc} is the maximal angle at which the calculation of the hydrodynamic equations does not yet give a shaped-charge jet. To determine φ_*^{calc}, we performed a series of calculations with a step of 2.5° in φ. The angle φ_*^{appr} introduced above, which bounds the region of existence of the approximate solution, is determined with an accuracy of 0.5°. For all cases given in Table 2, $\varphi_*^{\text{calc}} > \varphi_*^{\text{appr}}$, i.e., the approximate theory yields smaller values of φ_* for the jetless compression regime. For the problem of plate acceleration, the difference $\Delta\varphi = \varphi_*^{\text{calc}} - \varphi_*^{\text{appr}}$ varies within 3–5°. For the problem of compression by the impactor, despite the inhomogeneity of the flow incident on the point of contact, $\Delta\varphi$ has smaller values: from 3° for $v = 5$ km/sec to 1.5° for $v \geqslant 10$ km/sec. The passage through the critical value v_{cr}, for which the boiling liquid appear in the flow, does not influence $\Delta\varphi$.

For the problem of compression by the impactor for different v and φ, Table 3 gives the slope angle of the attached shock wave α, the angle β (see Fig. 2b), and the pressure and temperature behind the front of the attached wave obtained from calculations of the hydrodynamic equations and from the approximate solution

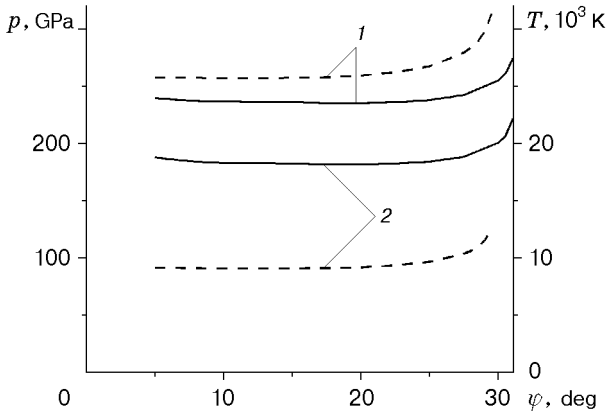

Fig. 5

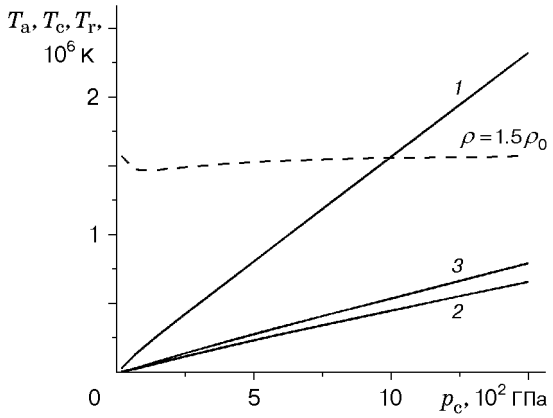

Fig. 6

Fig. 5. Pressure and temperature versus the angle φ (curves 1 and 2, respectively) in the approximate solution behind the attached wave for an aluminum plate ($v = 10$ km/sec): solid curves refer to compression by the impactor and dashed curves refer to acceleration.

Fig. 6. Temperature behind the fronts of the attached (T_a) and compression (T_c) waves and the wave reflected from the target (T_r) versus the pressure behind the front of the compression wave for compression of the plate of deuterium ice ($\varphi = 30°$) (curves 1, 2, and 3, respectively); the dashed curve shows the density behind the attached wave front related to the ice density.

(subscripts "calc" and "appr", respectively). The thermodynamic functions were determined near the point of attachment of the shock wave. With distance from the point of attachment, the values of the thermodynamic functions decrease. There is good (within 10%) agreement between the angular characteristics and pressures. The difference in temperature reaches 20%, which is apparently explained by the higher sensitivity of temperature to the accuracy of magnetohydrodynamic calculations. As in the case of determination of φ_*, the passage through v_cr does not influence the accuracy of the approximate solution.

Using the approximate solution, we consider in more detail the dependence of the thermodynamic functions behind the front of the attached shock wave on the parameters of the problem. Figure 5 gives the dependences of the pressure and temperature on the angle φ for the aluminum plate in the problems of acceleration and impact at $v = 10$ km/sec. It is evident that except in a small neighborhood of φ_*^appr, both functions depend weakly on φ. Since calculations using hydrodynamical equations do not confirm the increase in the thermodynamic functions near φ_*^appr, these functions can be considered independent of φ with an error of less than 10%.

We note that the temperatures for the two problems differ markedly. For shock-wave compression, the temperature is two times higher, which is due to the increase in the entropy of the flow incident on the point of contact.

For plate acceleration, the values of the thermodynamic functions behind the attached wave front coincide almost exactly with the values for head-on impact of the plate on the lead target. For shock-wave compression of the plate, the values behind the front of the attached wave differ markedly from the values behind the front of both the compression wave and the wave reflected from the target.

The high temperature behind the attached wave front T_a indicates that a thermonuclear reaction can be initiated by compression of a plate by a strong shock wave. Figure 6 gives the dependence of T_a on the pressure behind the compression wave front p_c for a plate of deuterium ice with a density of $\rho_0 = 0.175$ g/cm^3 and an initial temperature of 14 K. It is evident that the function $T_\mathrm{a}(p_\mathrm{c})$ is linear. For comparison, the figure gives the temperatures behind the fronts of the compression wave (T_c) and the wave reflected from the target (T_r), which also depend linearly on p_c and are about 3.5 times lower than T_a. At a pressure of $p_\mathrm{c} \approx 1500$ GPa, which is attainable on modern powerful laser systems, $T_\mathrm{a} > 2 \cdot 10^6$ K, which ensures a considerable rate of the (D–D) reaction.

Besides the temperature, the rate of the (D–D) reaction is also determined by the density of deuterium. Figure 6 gives the density ρ behind the front of the attached wave. It is evident that $\rho \approx 1.5\rho_0$ and is almost independent of p_c. This value is smaller than the density behind the front of a strong compression wave $\rho_c \approx 4\rho_0$.

Conclusion. For an aluminum plate accelerated or compressed by an aluminum impactor with a velocity of 5–15 km/sec, we obtained the critical values of the angle φ beginning with which the shaped-charge jet does not contain the boiling liquid.

For the jetless regime of shock-wave compression of the plate, we constructed an approximate solution with an attached shock wave that takes into account the phase composition of the plate material in the rarefaction wave. The approximate solution is in satisfactory agreement with the solution of the original problem. The thermodynamic functions behind the attached wave front are shown to depend weakly on the angle φ.

The temperature behind the attached wave front is severalfold higher than the temperature behind the front of the compression wave. The fundamental possibility of initiating a thermonuclear reaction is shown for jetless compression of a plate of deuterium ice by a strong shock wave.

We thank I. V. Lomonosov and K. V. Khishchenko for providing tables of the equations of state for aluminum, lead, and hydrogen.

This work was supported by the Russian Foundation for Fundamental Research (Grant No. 97-01-00095).

REFERENCES

1. A. V. Bushman, G. I. Kanel', A. L. Ni, and V. E. Fortov, *Thermal Physics and Dynamics of Intense Pulsed Actions* [in Russian], Inst. of Chem. Phys., USSR Acad. of Sci., Chernogolovka (1988).
2. J. M. Walsh, R. G. Shreffler, and F. J. Willig, "Limiting conditions for jet formation in high velocity collisions," *J. Appl. Phys.*, **24**, No. 3, 349–359 (1953).
3. E. I. Zababakhin and I. E. Zababakhin, *Phenomena of Unlimited Cumulation* [in Russian], Nauka, Moscow (1988).
4. G. E. Kuz'min and I. V. Yakovlev, "Collisions of metal plates with hypersonic velocity of the point of contact," *Fiz. Goreniya Vzryva*, **9**, No. 5, 746–753 (1973).
5. P. C. Chou, J. Carleone, and R. R. Karpp, "Criteria for jet formation from impinging shells and plates," *J. Appl. Phys.*, **47**, No. 7, 2975–2981 (1976).
6. S. A. Kinelovskii and Yu. A. Trishin, "Physical aspects of cumulation," *Fiz. Goreniya Vzryva*, **16**, No. 5, 26–40 (1980).
7. V. Ya. Ternovoi, "Jet formation by plasma compression in acute-angle geometry," *Prikl. Mekh. Tekh. Fiz.*, No. 5, 68–73 (1984).
8. A. A. Charakhch'yan, "Numerical investigation of deuterium implosion in a conical target with a strong shaped-charge effect," *Prikl. Mekh. Tekh. Fiz.*, **35**, No. 4, 22–32 (1994).
9. I. V. Lomonosov, A. A. Frolova, and A. A. Charakhch'yan, "Calculation of a high-velocity impact of a thin foil on a conical target," *Mat. Model.*, **9**, No. 5, 48–60 (1997).
10. A. A. Charakhch'yan, "Numerical investigation of circular cumulative jets compressing deuterium in conical targets," *Plasma Phys. Control. Fusion*, **39**, No. 2, 237–247 (1997).
11. A. A. Charakhch'yan, "Algorithms for calculating the decay of a discontinuity for the Godunov's scheme," *Zh. Vychisl. Mat. Mat. Fiz.*, **40**, No. 5, 782–796 (2000).
12. S. I. Anisimov, V. E. Bespalov, V. I. Vovchenko, et al., "Generation of neutrons during explosive initiation of the (D–D) reaction in conical targets," *Pis'ma Zh. Éksp. Teor. Fiz.*, **31**, No. 1, 67–70 (1980).
13. V. I. Vovchenko, I. K. Krasyuk, P. P. Pashinin, et al., "Pulsed compression and heating of a gas in conical targets," in: *Tr. IOFAN*, **36**, 5–82 (1992).
14. L. D. Landau and E. M. Lifshits, *Hydrodynamics* [in Russian], Nauka, Moscow (1986).